Hu et al.
*EURASIP Journal on Advances in Signal Processing* (2024) 2024:8
https://doi.org/10.1186/s13634-023-01102-2

EURASIP Journal on Advances in Signal Processing

RESEARCH **Open Access**

# Variable step size VLF/ELF nonlinear channel adaptive filtering algorithm based on Sigmoid function

Sumou Hu[1], Hui Xie[1*], Danling Liu[2] and Jie Hu[3]

*Correspondence: 0909031059@nue.edu.cn

[1] College of Electronic Engineering, Naval University of Engineering, Wuhan 430033, Hubei, People's Republic of China
[2] Yangtze River Wuhan Waterway Bureau, Wuhan 430033, Hubei, People's Republic of China
[3] College of Communication Engineering, Xidian University, Xi'an 710071, Shanxi, People's Republic of China

**Abstract**

The signals received by very low-frequency/extremely low-frequency nonlinear receivers are frequently affected by intense atmospheric pulse noise stemming from thunderstorms and global lightning activity. Current noise processing algorithms designed for nonlinear channels within these frequency ranges, which are predicated on fractional $p$-order moment alpha stable distribution criteria (where $0 < p < \alpha < 2$, and $p$ and $\alpha$ denote distinct characteristic indices of alpha stable distribution noise), are constrained by their reliance on limited $p$-order moment statistics. As a result, the performance of low-frequency nonlinear channel receivers experiences significant degradation when confronted with robust pulse noise interference ($0 < p < \alpha < 2$). To tackle this challenge, the present study introduces a novel variable step robust mixed norm (RMN) adaptive filtering algorithm, designated as SVS-RMN, which is based on the Sigmoid function. Leveraging the nonlinearity of the Sigmoid function and building upon the power function Hammerstein nonlinear channel model, the algorithm aims to enhance the RMN algorithm by deriving new cost functions and adaptive iteration formulas. The performance of the proposed algorithm is evaluated in comparison to conventional RMN algorithms based on fractional low-order moment (FLOM) criteria ($0 < p < 2$), as well as other algorithms employing variable step sizes and either FLOM or radial basis function (RBF) criteria, across various intensities of pulse noise and mixed signal-to-noise ratios. The experimental results reveal the following: (1) The proposed algorithm effectively mitigates strong pulse noise interference and significantly enhances the tracking performance of the RMN algorithm compared to conventional RMN algorithms based on FLOM criteria. (2) In terms of computational efficiency, simplicity of structure, convergence speed, and stability, the proposed algorithm surpasses other algorithms based on FLOM or RBF criteria.

**Keywords:** Very low-frequency/extremely low-frequency (VLF/ELF), Nonlinear channel, Strong pulse noise, Fractional low-order moment (FLOM), Sigmoid function

## 1 Introduction

The propagation properties of very low-frequency/extremely low-frequency (VLF/ELF) electromagnetic waves, operating in the 3 Hz to 30 kHz frequency range, yield low propagation loss when traversing diverse media such as seawater, rocks, and soil. These waves also demonstrate consistent amplitude and phase, facilitating deep penetration into seawater. Consequently, VLF/ELF electromagnetic waves play a crucial role in various engineering domains, encompassing wireless communication, submarine communication, underwater navigation, and seabed exploration [1–5].

In existing VLF/ELF nonlinear receivers, atmospheric noise poses a significant challenge due to its non-Gaussian pulse characteristics, characterized by suddenness, impulsiveness, and instantness. This noise serves as the primary interference factor affecting low-frequency signals. Experimental studies have confirmed that atmospheric noise in low-frequency channels can be well approximated by an alpha stable distribution noise model [6]. However, in practical applications, channel noise processing algorithms often need to distinguish between a specified sequence of Gaussian distributions ($\alpha=2$) or fractional lower-order moment alpha stable distributions ($\alpha<2$). When dealing with a sequence following a Gaussian distribution, which has a finite second-order moment (variance), the statistics beyond the second order cannot be accurately calculated in the presence of alpha stable distribution noise. Consequently, the performance of channel noise algorithms is compromised or rendered invalid when applied to Gaussian distribution scenarios [7–9].

To address the challenges posed by alpha stable distributed noise in adaptive filtering algorithms for linear time-invariant channel noise, Nikias and Shao [10] proposed the least mean $p$-norm (LMP) algorithm, which effectively suppresses alpha stable distributed noise. Building upon this work, several derivative algorithms have been proposed, including the stochastic gradient equalization algorithm (SGE) [11], normalized variable step size least mean $p$-norm algorithm (NVSS-LMP) [12], and variable step size least mean $p$-norm algorithm (VSS-LMP) [13]. While these methods notably enhance the performance of adaptive filtering for linear channels under alpha stable distribution noise, they require knowledge of the signal-to-noise ratio (SNR). As a result, their compensation ability for nonlinear channels under alpha stable distribution is limited, yielding unsatisfactory results.

An initial approach to tackle the denoising problem in nonlinear channels is to cascade multiple linear adaptive filters, with the Hammerstein-Wiener model [14] being a classic example. However, this approach remains fundamentally linear processing of a single filter and lacks the ability to effectively track more general nonlinear systems. Gabor [15] introduced Volterra sequences to address the challenges faced by nonlinear filtering, and Coker et al. [16] first applied Volterra series in the nonlinear channel adaptive filtering algorithm. To enhance the anti-pulse interference of Volterra filtering algorithms, Weng [17] introduced the nonlinear Volterra filtering LMP algorithm, which outperforms traditional Volterra least mean square (Volterra LMS) algorithms. In subsequent decades, to reduce algorithm complexity, scholars have proposed improved filtering algorithms based on the structure of the Volterra filter and Volterra filtering algorithm. These include second-order, third-order, and variable-step Volterra series least mean $p$-norm (Volterra LMP) algorithms [18–20]. While these approaches simplify the structure of the Volterra filter to some extent and reduce the complexity of Volterra series filtering algorithms, the complexity of Volterra series filtering algorithms remains high, making it difficult to meet the transmission quality requirements of nonlinear channels under alpha stable distribution noise.

Liu et al. [21] successfully introduced the radial basis function (RBF) criterion [22] into the LMS algorithm, resulting in the kernel least mean square (KLMS) algorithm. This algorithm, with its simple structure and ease of implementation, outperforms linear adaptive filtering algorithms in solving practical nonlinear problems. Building upon this, Gao et al. [23] proposed the kernel least mean $p$-norm (KLMP) algorithm, which has served as the foundation for subsequent research on improved algorithms. For instance, Dong [24] proposed the kernel fractional lower power (KFLP) algorithm for mitigating non-Gaussian pulse noise, based on fractional low-order statistical error criteria [25]. However, the KFLP algorithm suffers from slow convergence speed. To address this, Huo [26] introduced the variable scaling factor sigmoid kernel fractional lower power adaptive filtering algorithm based on the Sigmoid function (VS-SKFLP). By successfully combining the cost function of the KFLP algorithm with the neural network Sigmoid activation function inspired by biology [27–29], this algorithm significantly improves convergence speed and steady-state error. It is worth noting that these algorithms are all nonlinear channel adaptive filtering algorithms based on the RBF criterion in a Gaussian distribution environment. In the presence of mixed Gaussian and non-Gaussian noise interference, the RBF criterion requires more computation and exhibits weaker noise suppression.

To address the challenge of channel noise processing under the mixed interference of Gaussian and non-Gaussian noise, Chambers and Avlonitis [30] proposed the robust mixed-norm (RMN) algorithm, which combines error first- and second-order moments through convex combination. This algorithm improves the performance of fractional lower order moment (FLOM) criterion-based algorithms to some extent by incorporating the first-order moment. However, the convergence speed and steady-state performance remain insufficient. Papoulis and Stathaki [31] suggested adaptive changes to the fixed mixed parameters in the mixed-norm (MN) algorithm based on error and normalized step parameters in the weight coefficient update formula. These modifications significantly enhance the convergence speed and steady-state performance of the MN algorithm. Song and Zhao [32] proposed the reference signal filtered-x general MN (FxGMN) algorithm, which improves convergence speed through convex combination. The FxGMN algorithm's ability to control impact noise under different parameter combinations is studied. Yang [33] introduced a cost function based on mixed even moments with $0 < p < \alpha/2$.

In summary, VLF/ELF nonlinear receivers are susceptible to intense pulse noise ($0 < p < \alpha < 2$) in low-frequency signal noise. Many researchers have proposed various enhanced channel noise suppression algorithms based on FLOM or RBF criteria. However, in environments with high levels of pulse noise, the first-order moment (mean value, $p = 1$) and second-order moment statistics (variance, $p = 2$) of the channel noise become non-existent. This poses a significant challenge in effectively suppressing the noise, ultimately leading to failure or substantial performance degradation of the nonlinear receiver. Building upon the variable step neural network's Sigmoid activation function algorithm mentioned earlier, this paper introduces a variable step RMN algorithm based on the Sigmoid function (SVS-RMN). In this algorithm, the instantaneous error $e[n]$ of VLF/ELF signal noise is treated as a variable step size factor, leveraging the nonlinear properties of the Sigmoid function under different intensities of pulse noise and mixed Gaussian and non-Gaussian noise. Specifically, by adjusting the skew parameter $\eta$ of the Sigmoid function, the instantaneous error $e[n]$ of the RMN algorithm is adaptively controlled, enabling the acquisition of finite mean and variance of noise and effectively suppressing the discrete singularities caused by strong pulse noise in low-frequency signals. Compared to conventional RMN algorithms and other variable step-size $p$-order moment algorithms based on FLOM or RBF criteria, the SVS-RMN algorithm offers advantages such as a simple structure, low computation, fast convergence, and strong stability.

## 2 Alpha stable distribution noise properties

The alpha stable distribution is a significant model for representing non-Gaussian signals. In recent years, it has become evident that various types of noise, including ocean noise [34, 35], anthropogenic noise [36], clutter, and atmospheric noise in low-altitude environments [37–39], can be more accurately described by the alpha stable distribution. These types of noise display pronounced pulsating characteristics when compared to Gaussian noise. The alpha stable distribution is capable of generating noise with a longer tail than Gaussian noise, making it particularly well-suited for modeling pulse noise.

### 2.1 Characteristic function

Alpha stable distribution is commonly used to model pulse noise. The probability density function is not typically used to describe the distribution, but rather its characteristic function [40]. If a random variable $X$ follows an alpha stable distribution, denoted as $X \sim S_\alpha(\beta, \gamma, \delta)$, its characteristic function satisfies:

$$\varphi(u) = \exp\left\{ \mathrm{j}\delta u - \gamma |u|^\alpha [1 + \mathrm{j}\beta \operatorname{sgn}(u)\omega(u,\alpha)] \right\}, \tag{1}$$

in Eq. (1),

$$\omega(u,\alpha) = \begin{cases} \tan(\pi\alpha/2), \ \alpha \neq 1 \\ (2/\pi)\log|u|, \ \alpha = 1 \end{cases}, \tag{2}$$

$$\operatorname{sgn}(u) = \begin{cases} 1, & u > 0 \\ 0, & u = 0 \\ -1 & u < 0 \end{cases}. \tag{3}$$

In the above equations, $\alpha$, $\beta$, $\gamma$, and $\delta$ uniquely determine the characteristic function of the alpha stable distribution. $\alpha$ represents the characteristic index, where $\alpha = 2$ corresponds to a Gaussian distribution. As $\alpha$ decreases, the probability function of the alpha stable distribution becomes thicker, exhibiting stronger pulsing characteristics. This thick trailing property makes the alpha stable distribution suitable for describing actual noise with pulsing characteristics. $\beta$ is a symmetric parameter indicating the symmetry of the distribution, with a range of $-1 \leq \beta \leq 1$. A value of $\beta = 0$ indicates symmetry and is referred to as symmetric alpha stable distribution noise ($S\alpha S$). $\gamma$ is the dispersion coefficient, determining the extent of the probability density function's expansion. It is similar to the variance in Gaussian noise, with

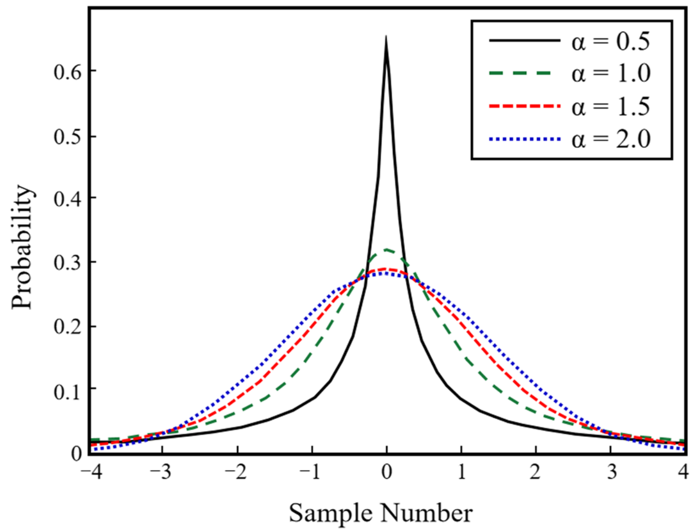


**Fig. 1** The impact of characteristic index $\alpha$ on the probability density function of stable distribution

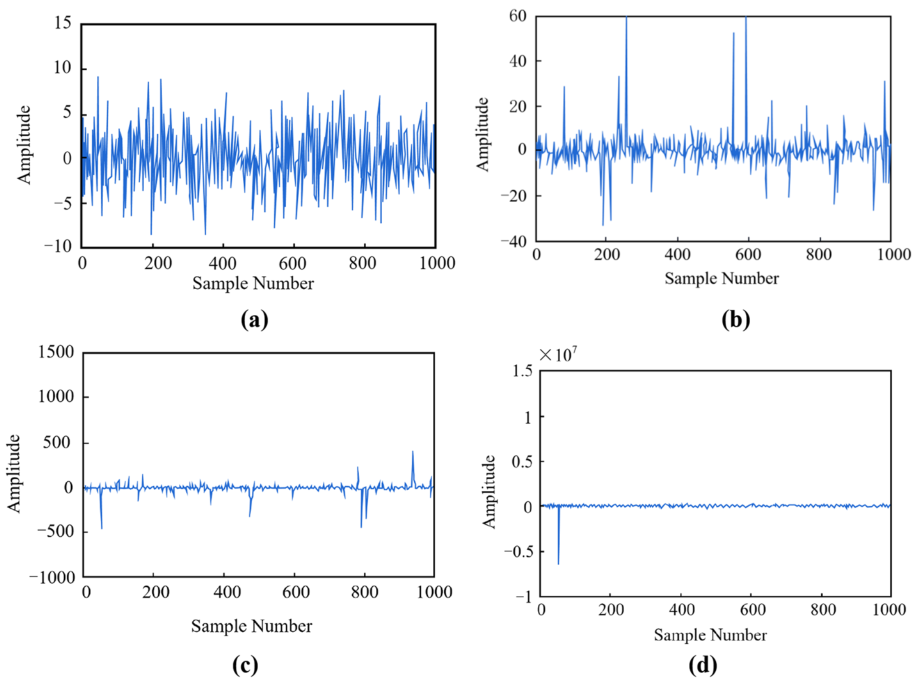


**Fig. 2** Variations in noise signal intensity for different alpha stable distributions. **a** $\alpha = 1.8$; **b** $\alpha = 1.5$; **c** $\alpha = 1.2$; **d** $\alpha = 0.5$

$\gamma \geq 0$. $\delta$ is a location parameter that represents the position of the probability density function on the $x$-axis, taking real number values. When $0 < \alpha < 2$, the non-gaussian stable distribution is referred to as the FLOA. Figures 1 and 2 illustrate the influence of the characteristic index $\alpha$ on the probability density function and alpha stable distributed noise signal, respectively, with varying intensity.

### 2.2 FLOM properties

The alpha stable distribution possesses several important properties, including its moment property. The statistical moments of noise provide valuable information about its characteristics [6, 7, 41]. The entire spectral distribution of statistical moments ranges from order 0 to infinite order, as depicted in Fig. 3. In general, the second moment of a random variable is usually defined as $E|X|^2$.

For an alpha stable distribution, higher-order moment statistics, including the second-order moment statistics, are non-existent. Consequently, the FLOM or lower-order distributed statistics play a crucial role. FLOM, represented as $E|X|^p$, where $0<p<\alpha\leq 2$, are specifically defined for random variables following an alpha stable distribution. The convergence properties of FLOM have been established through theorems [6, 7, 42], with proofs provided in [6]. Zolotareva [7] initially demonstrated these properties using the Mellin-Stieljes transformation, while Cambanis [43] offered a reproof based on characteristic function characteristics. According to these theorems, when the characteristic index of the alpha stable distribution is $0<\alpha<2$, only moments of order less than $\alpha$ are finite [6, 7, 40]. Significantly, signal processing methods that assume finite variance or second-order statistics, such as the least squares algorithm and RMN algorithm, will experience significant degradation and may yield inaccurate results. This highlights the challenge faced by traditional nonlinear channel adaptive filters in handling pulse noise.

## 3 Design and implementation of SVS-RMN algorithm

### 3.1 System identification model

The SVS-RMN algorithm for channel adaptive filtering aims to simultaneously input minimum shift keying (MSK) [44] signals corrupted by alpha stable distribution noise into both an unknown Hammerstein-type system [45–47] and an adaptive filter. The SVS-RMN algorithm is then employed to process the nonlinear data at the filter's output to obtain the optimal output signal. The block diagram of the system identification model for the nonlinear channel adaptive filter is shown in Fig. 4.

For an $M$-order finite impulse response (FIR) adaptive filter, the output at time $n$ is given [45]:

$$y[n] = S^{\mathrm{T}} W_{\mathrm{opt}} \tag{4}$$

where $S=[S(0), S(1), \ldots, S(n\text{-}1)]^{\mathrm{T}}$ and $W_{\mathrm{opt}}=[W_{\mathrm{opt}}(0), W_{\mathrm{opt}}(1), \ldots, W_{\mathrm{opt}}(n\text{-}1)]^{\mathrm{T}}$ represent the filter input signal vector and the optimal weight vector, respectively. The instantaneous error of the system's output is then calculated as:

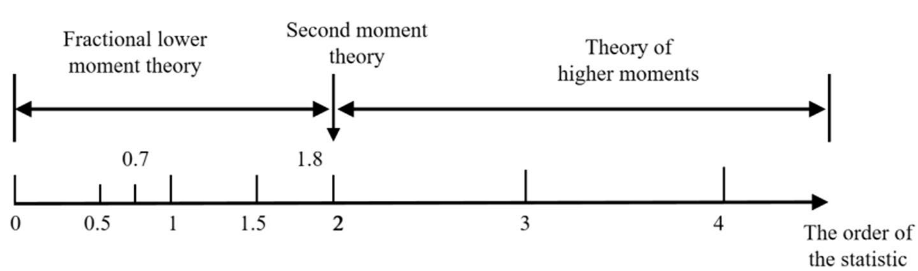


**Fig. 3** Diagram of moment distribution

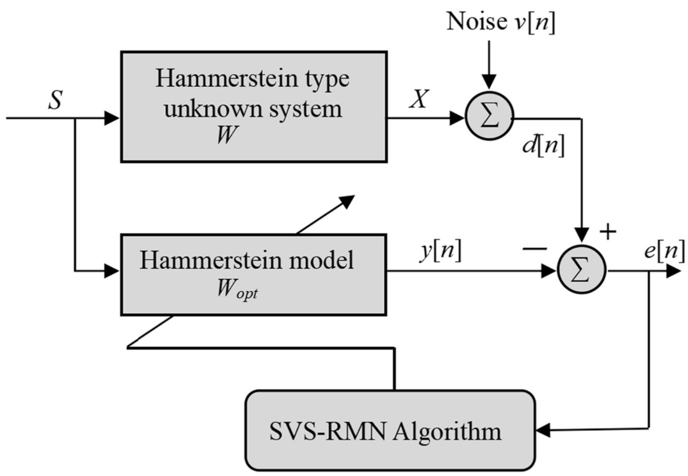


**Fig. 4** Block diagram of the system identification model for the SVS-RMN algorithm

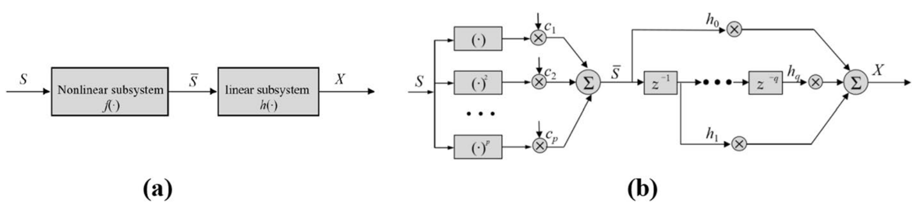


**Fig. 5** Block diagram of the Hammerstein nonlinear model of the power function class. **a** Subsystem structure; **b** System structure

$$e[n] = d[n] - y[\mathrm{n}] = d[n] - S^{\mathrm{T}} W_{\mathrm{opt}} \tag{5}$$

where $d[n] = S^{\mathrm{T}} W_{\mathrm{opt}} + e[n]$ represents the output signal of the unknown Hammerstein-type system, and $W_{\mathrm{opt}}$ is the optimal weight coefficient vector. The noise term $v[n]$ follows the FLOA.

The SVS-RMN channel adaptive filter proposed in this study employs a power function class Hammerstein nonlinear model, as shown in Fig. 5. The Hammerstein model consists of a nonlinear subsystem followed by a linear subsystem. The input signal $S$ and the output power function $X$ serve as the power functions of the Hammerstein nonlinear model.

Where $c_1, c_2, \ldots, c_p$ are the nonlinear coefficients, $h_0, h_1, \ldots, h_q$ are linear coefficients, $p$ represents the nonlinear order, $q$ is the linear memory depth. $f(\cdot)$ and $h(\cdot)$ represent the transmission function of the nonlinear subsystem and the impulse response of the linear subsystem respectively. Take the power function as an example, $f_m(\cdot) = (\cdot)^m$. $\overline{S}$ is a formal intermediate signal.

In this case, the Hammerstein nonlinear model of the power function class can be expressed as:

$$X = \sum_{k=0}^{q} h(k) \left( \sum_{m=1}^{p} c_m \overline{S}^m (n-k) \right). \tag{6}$$

The SVS-RMN algorithm, derived in this study, adaptively adjusts the Hammerstein filter until the responses of the two systems (as shown in Fig. 4) are equal to minimize the mean square error (MSE), as expressed in Eq. (7).

$$\mathrm{MSE}(k) = 10\log_{10}\left(\frac{1}{L+1}\sum_{n=k}^{k+L}|e[n]|^2\right) \tag{7}$$

where $L$ is the length of the input data.

### 3.2 Implementation of SVS-RMN algorithm

The conventional RMN algorithm has strong robustness to non-Gaussian pulse noise suppression. The cost function can be expressed as:

$$J(n) = \lambda(n)E|e[n]|^2 + [1-\lambda(n)]E|e[n]| \tag{8}$$

where $\lambda(n)$ is the mixed parameter. $E|e[n]|$ and $E|e[n]|^2$ represent the first- and second-order moments of the instantaneous error, respectively. The adaptive iteration formula is expressed as:

$$\begin{aligned} W(n+1) = W(n) + \mu\big\{\lambda(n)2e[n] + [1-\lambda(n)]\mathrm{sgn}(e[n])\big\} \\ (-2\eta\exp(-\eta e[n])S)/(1+\exp(-\eta e[n]))^2 \end{aligned} \tag{9}$$

where $\mu$ is the step factor used to control the convergence speed. Since the first-order moments $E|X|$ and second-order moments $E|X|^2$ of random variable $X$ are not finite under the condition of FLOA, we consider the variable-step method to improve the effectiveness of the algorithm.

The variable step size adaptive filtering algorithm, based on the Sigmoid function, operates on the principle that the instantaneous error can be considered as a variable factor influencing the step size through a nonlinear functional relationship. By adjusting the skew parameter $\eta$, the algorithm can adaptively modify the change in the instantaneous error $e[n]$ to achieve different convergence rates at different stages. In this section, the principle of variable step size adjustment will be introduced into the RMN algorithm based on the Sigmoid function, denoted as:

$$\mathrm{Sgm}(e[n]) = \frac{2}{1+\exp(-\eta e[n])} - 1, \quad \eta > 0 \tag{10}$$

where the parameter $\eta$ is the skew parameter, which is used to adjust the attenuation scale for different $e[n]$.

In the adaptive filtering algorithm, the instantaneous error function $e[n]$ is subject to FLOA, and its expression can be simplified as:

$$\begin{aligned} e[n] &= d[n] - S^{\mathrm{T}}W_{\mathrm{opt}} = X + v[n] - S^{\mathrm{T}}W_{\mathrm{opt}} \\ &= S^{\mathrm{T}}\left(W - W_{\mathrm{opt}}\right) + v[n] = S^{\mathrm{T}}U + v[n]. \end{aligned} \tag{11}$$

As can be seen from Fig. 4, $X=S^{\mathrm{T}}W$ in Eq. (11) represents the output signal of an unknown system of Hammerstein type. The weight coefficient error vector is denoted as $U=W\text{-}W_{\mathrm{opt}}$, and the system is optimized when the output $U$ is minimized. Based on the analysis conducted above, it is inferred that in the conventional RMN algorithm, when the channel noise $v[n]$ is FLOA, the second-order moment $E|e[n]|^2$ of the instantaneous error $e[n]$ becomes infinite when $\alpha < 2$, and the first-order moment $E|e[n]|$ of the instantaneous error $e[n]$ becomes infinite when $\alpha < 1$ [6, 7, 40, 42]. Therefore, the nonlinear property of the neural network Sigmoid function [29] is being considered for approximating these singular values.

The instantaneous error function $e[n]$ outputted by the RMN algorithm is transformed, and its expression can be given as follows:

$$\hat{e}[n] = \mathrm{Sgm}(e[n]) = \frac{2}{1 + e^{-\eta(e[n])}} - 1, \quad \eta > 0. \tag{12}$$

By substituting Eq. (11) into Eq. (12), the instantaneous error function after Sigmoid transformation yields finite values for $E|e[n]|$ and $E|e[n]|^2$. This information, along with the cost of the RMN algorithm, allows for the construction of a new cost function:

$$J(n) = \lambda(n)E\left|\hat{e}[n]\right|^2 + [1 - \lambda(n)]E\left|\hat{e}[n]\right|. \tag{13}$$

The impact of different sizes of the skew parameter $\eta$ on the cost function $J(n)$ is depicted in Fig. 6.

To minimize the cost function $J(n)$, the conjugate gradient with respect to the filter tap coefficient is computed, and the instantaneous gradient is used as a substitute for the true gradient, resulting in the following equation

$$\begin{aligned}\hat{\nabla}_W J(n) &= \left\{\lambda(n)2\hat{e}[n] + [1 - \lambda(n)]\mathrm{sgn}(\hat{e}[n])\right\}\partial\hat{e}[n]/\partial W \\ &= \left\{\lambda(n)2\hat{e}[n] + [1 - \lambda(n)]\mathrm{sgn}(\hat{e}[n])\right\}\partial(2/(1 + \exp(\eta e[n])) - 1)/\partial W \\ &= \left\{\lambda(n)2\hat{e}[n] + [1 - \lambda(n)]\mathrm{sgn}(\hat{e}[n])\right\}(-2\eta\exp(-\eta e[n]S)/(1 + \exp(-\eta e[n]))^2\end{aligned}. \tag{14}$$

The updated formula for the filter weight coefficient can be obtained by employing the steepest descent method.

$$W(n+1) = W(n) + \mu\hat{\nabla}_W J(\mathrm{n}). \tag{15}$$

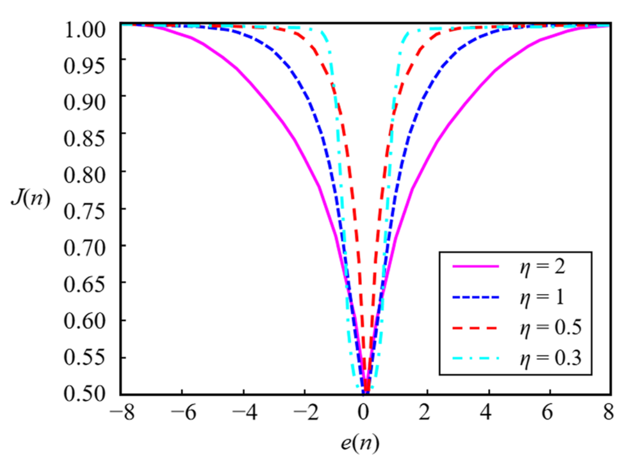


**Fig. 6** The impact of different sizes of the skew parameter $\eta$ on the cost function $J(n)$

By substituting Eq. (14) into Eq. (15), the adaptive iterative update formula can be obtained:

$$W(n+1) = W(n) + \mu\left\{\lambda(n)2\hat{e}[n] + [1-\lambda(n)]\mathrm{sgn}(\hat{e}[n])\right\} \\ (-2\eta\exp(-\eta e[n])S)/(1+\exp(-\eta e[n]))^2 . \tag{16}$$

Let the initialization $W(0) = \mathbf{0}$, after $k$ iterations, give the adaptive filter a new input signal $S$ can get the output signal of the filter.

By substituting Eq. (16) into the output signal $y[n] = S^{\mathrm{T}} W_{\mathrm{opt}}$, we derive the adaptive iterative equation for the SVS-RMN algorithm. In this paper, the selected Sigmoid function shares similarities with the RBF, enabling it to approximate any curve indefinitely and mitigate the impact of noise variations in low-frequency channels. The introduced Sigmoid function effectively approximates and transforms the signal singularity caused by pulse noise, and its inhibitory ability strengthens with increasing pulse noise intensity. This improvement addresses the issue of insufficient steady state or even failure of the RMN algorithm in FLOA environments, bringing the steady state error of the RMN algorithm closer to the actual value. Consequently, the anti-pulse interference capability of the RMN algorithm is significantly enhanced.

## 4 Simulation and analysis

### 4.1 Comparison of various pulse intensities

To evaluate the performance of the proposed SVS-RMN channel adaptive filtering algorithm, we conducted simulation experiments using a minimum frequency shift keying (MSK) modulation signal in a low-frequency communication system. The simulation experiments were conducted in nonlinear channels using a power function Hammerstein model, where the relationship between input and output is described by Eq. (6). The values of the nonlinear coefficient $c$ were set as 1, 0.25, and 0.125, respectively, and the values of the linear coefficient $h$ were set as 0.75, 0.035, and $-0.15$, respectively [45, 47]. We compared the performance of the SVS-RMN algorithm with that of the RMN, Volterra LMP, and VS-SKFLP algorithms under different noise pulse intensities. The MSE was used as a criterion to evaluate the performance of these algorithms, considering that the noise in the output signal of the filter has been suppressed. The MSE and mixed signal-to-noise ratio (MSNR) [45] are defined in Eqs. (7) and (17), respectively:

$$\mathrm{MSNR} = 10\log_{10}(\delta_s^2/\gamma_v). \tag{17}$$

Here $\delta_s{}^2$ represents the variance of the signal $S$, and $\gamma_{\mathrm{v}}$ is the dispersion coefficient of the alpha stable distribution noise. For the simulation, we assume the alpha stable distribution noise to be FLOA, without loss of generality.

To assess the adaptability of the proposed algorithm to alpha stable distributed noise, we conducted simulation experiments on the RMN, Volterra LMP, VS-SKFLP, and SVS-RMN algorithms under different noise pulse intensities, with MSNR set to 25 dB. We set $\alpha$ to 1.8, 1.5, and 1.2, respectively, and simulated the channel noise processing of the three algorithms using MATLAB software. The simulation parameters for each algorithm can be found in Table 1. The data in Table 1 represents the results of 200 independent runs, and a simulation diagram is provided in Fig. 7.

**Table 1** Simulation parameters for the four algorithms with $\alpha = 1.8$, 1.5, and 1.2

| | $\alpha = 1.8$ | $\alpha = 1.5$ | $\alpha = 1.2$ |
|---|---|---|---|
| SVS-RMN | $\mu = 0.035, \eta = 1$ | $\mu = 0.035, \eta = 1$ | $\mu = 0.035, \eta = 1$ |
| Volterra LMP [16] | $N_1 = 5, N_2 = 25$<br>$\mu = 3e{-}3, \mu = 5e{-}5$ | $N_1 = 5, N_2 = 25$<br>$\mu = 3e{-}3, \mu = 5e{-}5$ | $N_1 = 5, N_2 = 25$<br>$\mu = 3e{-}4, \mu = 5e{-}5$ |
| VS-SKLMP [26] | $\sigma = 5, \eta = 1$ | $\sigma = 4, \eta = 1$ | $\sigma = 4, \eta = 1$ |
| RMN [30] | $\mu = 0.0015$ | $\mu = 0.0015$ | $\mu = 0.0015$ |

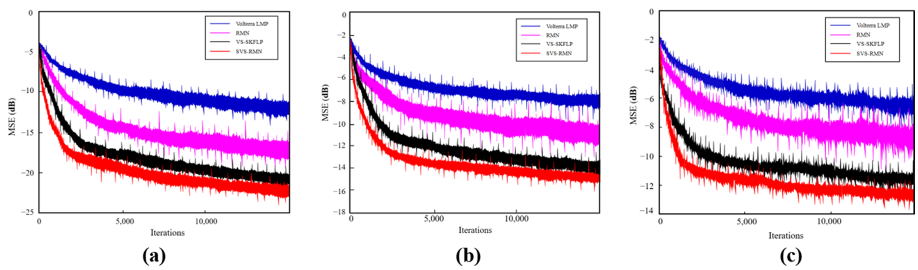


**Fig. 7** When MSNR= 25 dB, the MSE curves of the SVS-RMN algorithm and RMN, Volterra LMP and VS-SKFLP algorithms in this paper. **a** $\alpha = 1.8$; **b** $\alpha = 1.5$; **c** $\alpha = 1.2$

In the table, the symbols $\mu$, $N$ and $\sigma$ represent step factor, filter length and kernel parameter respectively, $\eta$ is the skew parameter of Sigmoid function; $\mu_1$ and $\mu_2$ represent the linear and nonlinear step sizes of the Volterra LMP, respectively. $N_1$ and $N_2$ represent the lengths of linear and nonlinear filters in the Volterra series adaptive filter, respectively.

As shown in Fig. 7, the SVS-RMN algorithm proposed in this study demonstrated robustness to the interference intensity of pulse noise, maintaining good performance even when the MSNR is 25 dB and $\alpha$ is 1.8, 1.5, and 1.2. It exhibited superior convergence speed and steady-state error compared to the RMN, Volterra LMP, and VS-SKFLP algorithms. The proposed algorithm outperformed traditional RMN and Volterra LMP algorithms based on the FLOM criterion, reducing the steady-state error by an average of 6 dB and 12 dB, respectively, while also improving convergence speed and steady-state error performance. The proposed algorithm exhibited stronger resistance to pulse interference. It is important to note that MSE results do not necessarily mean an increase in either symbol- or bit-error rates. Additionally, it was observed that for iterations greater than 10,000, the proposed algorithm overlapped with the VS-SKFLP algorithm based on the RBF criterion in certain areas. This consistency in the MSE change curve validates the correctness of the proposed method.

The reasons can be explained as follows:

1. The proposed SVS-RMN method effectively resolves the failure issue encountered by RMN, Volterra LMP, and VS-SKFLP algorithms in the presence of FLOA pulse interference. As the intensity of pulse interference increases, the performance of RMN, Volterra LMP, and VS-SKFLP algorithms is adversely affected. However, SVS-RMN demonstrates minimal susceptibility to pulse intensity and achieves superior balancing effects.

2. In contrast to the traditional RMN algorithm, the method proposed in this paper resolves the issue of non-existent statistics of the first- and second-order moments in the RMN algorithm's solution for FLOA. The proposed method allows for adaptive adjustment of the step size factor to accommodate varying intensity levels of pulse noise in different channel noise environments, thereby significantly enhancing the tracking performance of the RMN algorithm.
3. When compared to VS-SKFLP and Volterra LMP, the VS-SKFLP system based on RBF criteria exhibits a complex structure and requires more than two multiplications. Additionally, the step factor updating in Volterra LMP necessitates multiple operations, and the operations of Volterra sequence increase exponentially. On the other hand, the proposed SVS-RMN algorithm only requires a single multiplication operation, resulting in a simpler system, faster computation speed, and accelerated convergence.

### 4.2 Comparison of MSNR at different intensities

To further verify the effectiveness of the proposed algorithm in multipath weakened channels with different MSNR, the power function class Hammerstein model nonlinear channel was considered. The performance of the SVS-RMN algorithm was compared with the RMN, Volterra LMP, and VS-SKFLP algorithms, with the MSNR set to 15 dB and 0 dB, as shown in Fig. 8.

The results showed that the SVS-RMN algorithm effectively mitigates the influence of MSNR changes in the channel, accelerating the convergence speed while maintaining a low steady-state error. In contrast, the RMN, Volterra LMP, and VS-SKFLP algorithms were more susceptible to MSNR changes, with the MSE curve of the Volterra LMP and RMN algorithms exhibiting the most significant changes. This may be attributed to the inability of these algorithms to effectively extract useful signals and suppress noisy signals in complex noise environments.

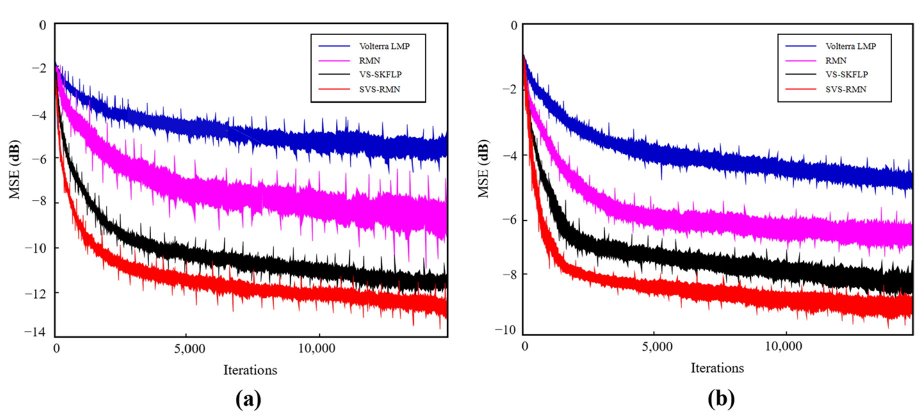


**Fig. 8** When $\alpha = 1.5$ and MSNR are 15 dB and 0 dB respectively, the performance of the proposed algorithm is compared with RMN, Volterra LMP and VS-SKFLP algorithms. **a** MSNR = 15 dB; **b** MSNR = 0 dB

## 5 Conclusion

In this research, we have proposed the SVS-RMN nonlinear channel adaptive filtering algorithm based on the power function Hammerstein model. The introduction of the Sigmoid function optimizes the traditional RMN algorithm, resulting in derived cost functions and adaptive iteration formulas for the SVS-RMN algorithm. Experimental comparisons with the traditional RMN, Volterra LMP, and VS-SKFLP algorithms validate the superiority of the proposed algorithm. The simulation results demonstrate the following: (1) The proposed algorithm outperforms other RMN algorithms based on the FLOM criterion, Volterra LMP algorithm, and VS-SKFLP algorithm based on RBF criterion in terms of convergence speed, stability error performance, and computational efficiency under different intensities of pulse noise and mixed noise interference. (2) Compared to the traditional RMN algorithm, the proposed algorithm achieves a reduction in steady-state error by approximately 6 dB, significantly improving the signal tracking performance of the original RMN algorithm in the presence of strong pulse noise. Thus, the proposed algorithm provides a new approach for suppressing noise in nonlinear receivers operating in VLF/ELF channels.

**Abbreviations**

| | |
|---|---|
| VLF/ELF | Very low frequency/extremely low frequency |
| MN | Mixed norm |
| FLOA | Fractional lower order moment Alpha stable distribution |
| SVS-RMN | Sigmoid function with variable step robust mixed norm |
| FLOM | Fractional low-order moment |
| LMP | Least mean *p*-norm |
| VSS-LMP | Variable step size least mean p-norm |
| SNR | Signal-to-noise ratio |
| LMS | Least mean square |
| KLMS | Kernel least mean square |
| KLMP | Kernel least mean *p*-norm |
| KFLP | Kernel fractional lower power |
| SGE | Stochastic gradient equalization algorithm |
| NVSS-LMP | Normalized variable step size least mean *p*-norm algorithm |
| VS-SKFLP | Variable scaling factor sigmoid kernel fractional lower power |
| Volterra LMP | Volterra series least mean *p*-norm algorithm |
| MDC | Minimum dispersion coefficient |
| RMN | Robust mixed-norm |
| FxGMN | Filtered-x general MN |
| SαS | Symmetric alpha stable distribution |
| FIR | Finite impulse response |
| RBF | Radial basis function |
| MSE | Minimum mean square error |
| MSK | Minimum frequency shift keying |

**Acknowledgements**
The authors express their gratitude to the editor and anonymous reviewers for their insightful comments and valuable suggestions. The authors would also like to acknowledge the support and assistance provided by the Communications Engineering Laboratory, Naval University of Engineering, Wuhan, China.

**Author contributions**
All authors are involved in deriving the algorithm and making the validation experiments. All authors read and approved the final manuscript.

**Funding**
The authors declare that this manuscript have no fund support.

**Availability of data and materials**
The data that support the findings of this study are available from the corresponding author on reasonable request.

## Declarations

**Ethics approval and consent to participate**
Not applicable.

**Consent for publication**
All authors declare that the manuscript consents to publication.

**Competing interests**
The authors declare that they have no conflicts of interest.

Received: 10 April 2023 Accepted: 21 December 2023
Published online: 06 January 2024

### References

1. H. Rowe, Extremely low frequency communication to submarines. IEEE Trans. Commun. **22**(4), 371–386 (1974)
2. A.B.M. Yusof, S. Kabir, An overview of sonar and electromagnetic waves for underwater communication. IETE Tech. **29**, 307–317 (2012)
3. J. Macnae, Stripping very low frequency communication signals with minimum shift keying encoding from streamed time-domain electromagnetic data. Geophysics **80**(6), E343–E353 (2015)
4. H. Xie, X.Y. Xu, H.N. Wu, N. Wang, Multiobjective particle swarm optimization to design the top load of a very low frequency thirteen-tower umbrella antenna. Int. J. RF Microw. Comput. Aided Eng. **2023**, 1792918 (2023)
5. S.M. Hu, H. Xie, T. Ding, Electromagnetic field variation of ELF Near-region excited by HED in a homogeneous Half-space model. Appl. Sci. **13**(13), 7499 (2023)
6. C.L. Nikias, M. Shao, *Signal Processing with Alpha-Stable Distributions and Applications* (Wiley, New York, 1995)
7. B. Chen, L. Xing, H. Zhao, N. Zheng, J.C. Príncipe, Generalized correntropy for robust adaptive filtering. IEEE Trans. Signal Process. **64**(13), 3376–3387 (2016)
8. J. Zhao, H. Zhang, J.A. Zhang, Generalized maximum correntropy algorithm with affine projection for robust filtering under impulsive-noise environments. Signal Process. **172**, 107524 (2020)
9. Y. Zhang, Y. Zhao, G. Wang, X. Rui, Mean square cross error: performance analysis and applications in non-Gaussian signal processing. EURASIP J. Adv. Signal Process. **24**(2021), 1–20 (2021)
10. M. Shao, C.L. Nikias, Signal processing with fractional lower order moments: stable processes and their application. Proc. IEEE **81**(7), 986–1010 (1993)
11. Y.L. Hao, Z.M. Shan, F. Shen, Gradient-norm based VSS-NLMP algorithm in $\alpha$-stable environments. Syst. Eng. Electron. **34**(4), 5–10 (1993)
12. M.T. Akhtar, A time-varying normalized step-size based generalized fractional moment adaptive algorithm and its application to ANC of impulsive sources. Appl. Acoust. **155**, 240–249 (2019)
13. B. Wang, H.Q. Li, S.J. Gao, M.L. Zhang, C. Xu, A variable step size least mean $p$-power adaptive filtering algorithm. J. Electron. Inf. Technol. **44**(2), 661–667 (2022)
14. N. Wiener, *Nonlinear Problems in Random Theory* (Wiley, New York, 1958)
15. D. Gabor, Holographic model of temporal recall. Nature **217**(5128), 584 (1968)
16. M. Coker, D. Simkins, A nonlinear adaptive noise canceller, in: *Acoustics, Speech, and Signal Processing, IEEE International Conference on ICASSP* (1980), pp. 470–473
17. B.W. Weng, K.E. Barner, Nonlinear system identification in impulsive environments. IEEE Trans. Signal Process. **53**(7), 2588–2594 (2005)
18. P.P. Yan, Z.J. Zhao, J.N. Shang, Z.D. Zhao, Variable memory length LMP algorithm of second-order Volterra filter. Comput. Eng. Appl. **3**, 121–125 (2013)
19. Y. Liu, Z.A. Di, A new variable step-size non-linear satellite channel equalization algorithm based on FLOM. J. Comput. Appl. **36**(S2), 11–13 (2016)
20. T.Y. Cui, J. Zhang, X.L. Huang, A variable step size Volterra LMP algorithm and its application for reducing noise of engine. J. Changchun Normal Univ. **41**(2), 57–62 (2022)
21. W. Liu, P.P. Pokharel, J.C. Principe, The kernel least-mean-square algorithm. IEEE Trans. Signal Process. **56**(2), 543–554 (2008)
22. L. Janjanam, S.K. Saha, R. Kar, D. Mandal, Global gravitational search algorithm-aided Kalman filter design for Volterra-based nonlinear system identification. Circuits Syst. Signal Process. **40**, 2302–2334 (2021)
23. W. Gao, J. Chen, Kernel least mean $p$-power algorithm. IEEE Signal Process. Lett. **24**(7), 996–1000 (2017)
24. Q. Dong, Y. Lin, Kernel fractional lower power adaptive filtering algorithm against impulsive noise. Comput. Sci. **S2**, 90–92 (2019)
25. S.-C. Pei, C.-C. Tseng, Least mean $p$-power error criterion for adaptive FIR filter. IEEE J. Sel. Areas Commun. **12**(9), 1540–1547 (1994)
26. Y.L. Huo, D.F. Wang, X.Q. Long et al., A variable-scale S-type kernel fractional low-power adaptive filtering algorithm. Acta Phys. Sin. **70**(15), 158401 (2021)
27. S.J. Han, F.Q. Tian, Derivation of a sigmoid generalized complementary function for evaporation with physical constraints. Water Resour. Res. **54**, 1734–1736 (2018)
28. S. Elfwing, E. Uchibe, K. Doya, Sigmoid-weighted linear units for neural network function approximation in reinforcement learning. Neural Netw. **107**, 3–11 (2018)
29. X. Zhao, G. Plata, P.D. Dixit, SiGMoiD: a super-statistical generative model for binary data. PLoS Comput. Biol. **17**(8), e1009275 (2021)
30. J. Chambers, A. Avlonitis, A robust mixed-norm adaptive filter algorithm. IEEE Signal Process. Lett. **4**(2), 46–48 (1997)

31. E.V. Papoulis, T. Stathaki, A normalized robust mixed-norm adaptive algorithm for system identification. IEEE Signal Process. Lett. **11**(1), 56–59 (2004)
32. P. Song, H.Q. Zhao, Filtered-x generalized mixed norm (FXGMN) algorithm for active noise control. Mech. Syst. Signal Process. **107**, 93–104 (2018)
33. B.H. Yang, An adaptive filtering algorithm for non-Gaussian signals in alpha-stable distribution. Traitement du Signal **37**(1), 69–75 (2020)
34. M. Bouvet, S.C. Schwartz, Comparison of adaptive and robust receivers for signal detection in ambient underwater noise. IEEE Trans. Acoust. Speech Signal Process. **37**(5), 621–626 (1989)
35. A.Q. Zhang, T.S. Qiu, X.H. Zhang, A new underwater acoustic signals processing approach to a-stable distribution. J. Electron. Inf. Technol. **27**(8), 1201–1204 (2005)
36. D. Middleton, Statistical-physical models of electromagnetic interference. IEEE Trans. Electromagn. Compat. **19**(3), 106–127 (1977)
37. E. Field, M. Lewinstein, Amplitude-probability distribution model for VLF/ELF atmospheric noise. IEEE Trans. Commun. **26**(1), 83–87 (1978)
38. A.A. Giordano, F. Haber, Modeling of atmospheric noise. Radio Sci. **7**(11), 1011–1023 (1972)
39. M. Shinde, S. Gupta, Signal detection in the presence of atmospheric noise in tropics. IEEE Trans. Commun. **22**(8), 1055–1063 (1974)
40. G. Samoradnitsky, *Stable Non-Gaussian Random Processes: Stochastic Models with Infinite Variance*, 1st edn. (Routledge, New York, 1994)
41. F.W. Machell, C.S. Penrod, G.E. Ellis, *Statistical Characteristics of Ocean Acoustic Noise Processes* (Springer, New York, 1989)
42. X.Y. Ma, C.L. Nikia, Parameter estimation and blind channel identification in impulsive signal environments. IEEE Trans. Signal Process. **43**(12), 2884–2897 (1995)
43. S. Cambanis, G. Miller, Linear problems in pth order and stable processes. SIAM J. Appl. Math. **41**(1), 43–69 (1981)
44. S.M. Hu, J.K. Tu, Application of SC-FDE equilibrium technology based on MSK modulation signal. Commun. Technol. **54**(11), 2564–2568 (2021)
45. A. Hammerstein, Nichtlineare Integralgleichungen nebst Anwendungen. Acta Math. **54**(1), 117–176 (1930)
46. S. Singh, T.K. Rawat, A. Ashok, Nonlinear system identification using butterfly optimisation algorithm and Hammerstein model. Int. J. Model. Identif. Control. **42**(2), 171–179 (2023)
47. S. Singh, A. Ashok, T.K. Rawat, Optimal Volterra-based nonlinear system identification using arithmetic optimization algorithm assisted with Kalman filter. Evol. Syst. **14**(1), 117–139 (2023)


## Publisher's Note

Springer Nature remains neutral with regard to jurisdictional claims in published maps and institutional affiliations.